Thermal Spray 2022: Proceedings from the International Thermal Spray Conference
May 4-6, 2022; Vienna, Austria
https://doi.org/10.31399/asm.cp.itsc2022p0907

Assessment of High Entropy Alloys as Thermally Sprayed Heating Elements

K. Bobzin, H. Heinemann, A. Schacht

An efficient temperature control on tool surfaces is essential in processes like injection moulding or die casting. A thermally sprayed heating coating could combine dynamic heating properties with a small assembly space as it is sprayed directly onto the cavity surface. With their intrinsically high electrical resistivity and low thermal expansion as compared with traditional alloys, High Entropy Alloys (HEA) show promising properties for the use as heating elements. Thus, the well-studied HEA $Al_{0.5}CoCrFeNi$ was used as a starting material for additional alloying with Zr and Si to force further lattice distortion in the solid solution. HEAs of differing compositions were melted and characterized. In the process, the potential of HEAs was assessed by characterizing their phase composition, thermal stability, and electrical resistivity. The characterized HEAs show a solid solution mainly consisting of fcc and bcc structure. Moreover, the composition $Al_{0.5}CoCrFeNiZr_{0.2}Si_{0.2}$ was determined as stable after heat treatment at 600 °C for 324 h. In addition, the electrical resistivity was raised by over 20 % relative to the starting material. As a result, a hitherto unknown HEA composition was detected to possess superior properties to traditional alloys for the application as heating coating.

1 Introduction

Variotherm moulding tools are used to improve parts quality through combining two temperatures within one production cycle. During or before the injection phase, the mould is heated to improve the flowability of the melt. After the mould is filled, the temperature needs to be reduced to allow for a quick solidification of the melt. Conventional methods include fluid-based systems, induction and radiation heating. In fluid-based systems the whole moulding tool is heated and cooled through heat conduction [1]. The other methods allow for rapid heating of the cavity surface, but only while the tool is opened. These conventional methods either lack dynamics in temperature change like fluid-based systems or require additional process steps. To improve the temperature control within the moulding process, heating coatings could become an alternative as they can be applied on the tool surface and provide heat exactly where it is needed.

Thermal spraying is an auspicious way of applying such heating coatings onto moulding tools. With its wide variation of processible coating materials, complete heating coating systems made of insulating and electrically conductive materials can be manufactured by using only one technology. The general use of thermally sprayed heating coatings was published in the past several time dating back to 1995, where Fasching et al. demonstrated a thermally sprayed coating system including a metallic heater [2]. Intense research on metallic heating coatings from Ni and NiCr20 has been conducted by Prudenziati et al. [3,4]. The heat generation is tied to the electrical resistance of the heating coating, thus ceramic heating coatings are a competitive alternative to metallic heaters. One particular ceramic material in focus of studies on heating coatings is the suboxide of TiO_2, which was investigated as a heating coating by Floristán et al. [5] and Scheitz et al. [6]. While all these investigation have focussed on the general use of thermal spraying for heating coatings, the authors have demonstrated the feasibility [7] as well as the actual implementation of TiO_x/Cr_2O_3 heating coatings in injection moulding processes [8].

Thermally sprayed metallic heating coatings have lower electrical resistivity compared to ceramic coatings, which leads to them being less effective in heating. The dissipated Joule heating, which is utilized to generate heat, is directly proportional to the electrical resistance. To achieve a sufficient total electrical resistance of the heating coating, metallic coatings have to be applied as thin and long conductor paths limiting the geometrical freedom in their design [6]. However, metals usually exhibit a less brittle behaviour than ceramics. High Entropy Alloys (HEA) are an innovative class of metals, which usually consist of a minimum of five metallic element in equal or near-equal atomic concentrations [9]. Due to strong lattice distortion in HEA, a higher electrical resistivity can be achieved, if compared to conventional metals and alloys [10]. Therefore, the geometrical limitations in the use as heating coatings could be reduced. Despite promising possibilities of HEA for application in heating elements, not many studies are conducted on the determination of electrical properties of HEA. One exception is the study by Chou et al., which has shown that the electrical resistivity of $Al_xCoCrFeNi$ ($0 \leq x \leq 2$) can reach the value of $\rho = 160\ \mu\Omega\cdot cm$ [11]. In another study by Kao et al. the electrical resistivity of $Al_{0.5}CoCrFeNi$ in the as-cast state was found to be $\rho = 135\ \mu\Omega\cdot cm$ [12]. These are competitive values compared to the electrical resistivity of NiCr20 and FeCrAl, which have an electrical resistivity between $\rho = 110\ \mu\Omega\cdot cm$ and of $\rho = 140\ \mu\Omega\cdot cm$ [13] and are often used in heating elements.

In previous studies at IOT, the oxidation behaviour [14] and the mechanical properties [15] of $Al_{0.6}CrFeCoNi$ and $Al_{0.6}CrFeCoNiSi_{0.3}$ as well as the wear resistance corresponding sprayed coatings were studied, demonstrating the beneficial properties of HEA. In this study, $Al_{0.5}CoCrNiFe$ was used as a reference HEA as its electrical properties are well studied among HEA as listed above. The aim was to develop an alloy with an electrical resistivity of more

than ρ > 140 µΩ·cm, which is larger than the electrical resistivity of the commonly used alloys, NiCr20 and FeCrAl. Lattice distortion is stated to be one major impact factor for the unique properties of HEA [10]. Thus, severe lattice distortion was evoked within the lattice of $Al_{0.5}CoCrNiFe$ to achieve an increase of the alloy's electrical resistivity. Therefore, Zr with relatively larger and Si with relatively smaller atomic size than the initial elements' atomic sizes were alloyed into the well-known HEA $Al_{0.5}CoCrNiFe$. Furthermore, the thermal stability of the alloys was investigated to evaluate their prospective application as heating elements.

2 Methods and materials

Mixtures of powders and granulates were prepared according to the atomic ratios of $Al_{0.5}CoCrNiFeZr_xSi_y$ with $0 \leq x \leq 0.5$ and $0 \leq y \leq 0.2$. A full list of the investigated 13 HEA is summarized in **Table 1**. Elemental powders by Goodfellow Cambridge Ltd, Huntingdon, United Kingdom, with particle sizes between 45 µm and 250 µm and purities of more than 99 % as well as Zr granulate by Chempur GmbH, Karlsruhe, Germany, with particle size between 1 mm and 3 mm and a purity of 99.8 % were used in preparation of HEAs. Zr was used as granulate to reduce its effective surface for inevitable oxidation during its handling. After mixing, the specimens were remelted within the vacuum furnace MOV 553T by PVA TePla AG, Wettenberg, Germany, into ingots. Each specimen was prepared to weigh 8 g and was filled in cylindrical Al_2O_3 crucibles. The remelting was done at 1,300 °C for 2 h followed by a slow cooling within the closed furnace until room temperature. To prevent the volatilization of elements, a flowing Ar atmosphere of 40 mbar was applied. This melting procedure has been found to be insufficient for some compositions. For specimens, which were not remelted, but only sintered, the induction coil within the melt spinning plant MSP10 by Edmund Bühler GmbH, Bodelshausen, Germany, was utilized to achieve remelting at higher temperatures than 1,300 °C, if necessary. The melt spinning plant was also used for production of HEA tapes to estimate possible changes in properties due to high cooling rates, which occur in the actual process of thermal spraying.

Table 1. Nominal atomic ratio of the investigated HEA compositions with their corresponding mass proportions within the powder mixtures.

Nominal atomic ratio	Al [wt.-%]	Co [wt.-%]	Cr [wt.-%]	Fe [wt.-%]	Ni [wt.-%]	Zr [wt.-%]	Si [wt.-%]
$Al_{0.5}CoCrFeNi$	5.9	24.6	21.7	23.3	24.5	-	-
$Al_{0.5}CoCrFeNiZr_{0.2}$	5.4	22.9	20.2	21.7	22.8	7.1	-
$Al_{0.5}CoCrFeNiZr_{0.2}Si_{0.1}$	5.4	22.6	20.0	21.4	22.5	7.0	1.1
$Al_{0.5}CoCrFeNiZr_{0.2}Si_{0.2}$	5.3	22.4	19.8	21.2	22.3	6.9	2.1
$Al_{0.5}CoCrFeNiZr_{0.3}$	5.2	22.1	19.5	20.9.	22.0	10.3	-
$Al_{0.5}CoCrFeNiZr_{0.3}Si_{0.1}$	5.2	21.9	19.3	20.7	21.8	10.1	1.0
$Al_{0.5}CoCrFeNiZr_{0.3}Si_{0.2}$	5.1	21.6	19.1	20.5	21.6	10.0	2.1
$Al_{0.5}CoCrFeNiZr_{0.4}$	5.1	21.4	18.8	20.2	21.3	13.2	-
$Al_{0.5}CoCrFeNiZr_{0.4}Si_{0.1}$	5.0	21.1	18.7	20.0	21.1	13.1	1.0
$Al_{0.5}CoCrFeNiZr_{0.4}Si_{0.2}$	5.0	20.9	18.5	19.8	20.8	13.0	2.0
$Al_{0.5}CoCrFeNiZr_{0.5}$	4.9	20.7	18.2	19.6	20.6	16.0	-
$Al_{0.5}CoCrFeNiZr_{0.5}Si_{0.1}$	4.9	20.5	18.1	19.2	20.4	15.9	1.0
$Al_{0.5}CoCrFeNiZr_{0.5}Si_{0.2}$	4.8	20.3	17.9	19.2	20.2	15.7	1.9

As the alloys are developed aiming for the application as heating elements, the phase stability over time at elevated temperatures in air is of utmost importance. To address that aspect, thermal aging was conducted in air at 600 °C for 24 h, then 100 h and finally 200 h for a cumulative time of 324 h per specimen. During this step, the chamber furnace N100/14 by Nabertherm GmbH, Lilienthal, Germany, was used. The phase composition was determined by means of X-ray diffraction (XRD). The measurements was performed on the specimens after remelting in the as cast state and again after thermal aging to detect any thermally induced phase change. Using the XRD 3000 by Waygate Technologies, Hürth, Germany, a Cu X-ray tube was operated at 40 mA and 40 kV within a scan range of $30° \leq 2\theta \leq 90°$ with a scanning speed of 6 s per step and step width of 0.05°. In post-processing, all measurements were normalized to their maximum peak.

The electrical resistance of the specimens was measured in the as cast state by four-wire sensing with the milliohm meter ILOM-508A by Isothermal Technology Ltd, Southport, United Kingdom. For the four-wire sensing, each specimen was cut to a cuboid shape of approximately 6 mm in length, 5 mm in width and 2 mm in height. To reduce measurement errors, the arithmetical average of 14 individual measurements was taken. Then the electrical resistivity was calculated considering each specimen's dimensions.

3 Results and discussion

All 13 compositions were manufactured successfully as ingots. The composition $Al_{0.5}CoCrFeNi$ had to be remelted with the induction coil as the temperature of 1,300 °C was not sufficient to melt this alloy completely. The XRD analyses of $Al_{0.5}CoCrFeNi$, $Al_{0.5}CoCrFeNiZr_{0.5}$ and $Al_{0.5}CoCrFeNiZr_{0.2}Si_{0.2}$ in the as-cast state are given in Figure 1. $Al_{0.5}CoCrFeNi$ shows an XRD spectrum congruent to reported measurements by Chou et al. [11] and Wang et al. [16]. It consists mainly of an fcc phase with a minor proportion of bcc phase. The addition of 16 wt.-% Zr induces a significant distortion of the fcc lattice in $Al_{0.5}CoCrFeNiZr_{0.5}$ resulting in a significant shift of its diffraction peaks. Furthermore, the proportion of bcc is larger than fcc and small amounts of a tetragonal phase, which seems to be a CrFe-rich phase according to the JCPDS card 01-071-7530, are formed. In $Al_{0.5}CoCrFeNiZr_{0.2}Si_{0.2}$, the addition of 6.9 wt.-% Zr together with 2.1 wt.-% Si only leads to an insignificant distortion of the fcc phase, while keeping the proportion between fcc and bcc at a similar level as in $Al_{0.5}CoCrFeNi$. These observations are a first identifier for the intended lattice distortion caused by Zr and Si and promise improved electrical resistivity for these alloys.

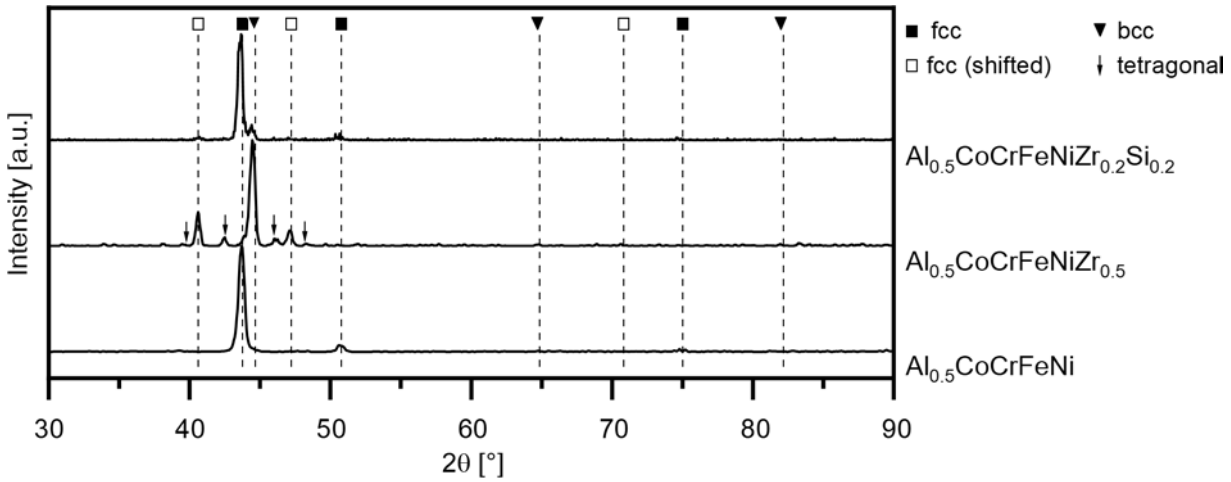

Figure 1. XRD analyses of selected $Al_{0.5}CoCrFeNiZr_xSi_y$ alloys in as-cast state.

Observing the electrical resistivity of $Al_{0.5}CoCrFeNiZr_xSi_y$ alloys compared to the reference without Zr or Si addition in Figure 2, a significant increase stands out. The electrical resistivity of the composition $Al_{0.5}CoCrFeNi$ was determined to be ρ = 130.5 µΩ·cm, which is within experimental error of the value of ρ = 135 µΩ·cm reported by Kao et al. [12] for the as-cast alloy. From the reference value of ρ = 130.5 µΩ·cm, a minimum increase of 10 % and a maximum increase of 26 % was detected resulting in ρ = 144.5 µΩ·cm and ρ = 164.5 µΩ·cm, respectively. The electrical resistivity shows a clear dependency to the Zr content. However, the addition of Si does not affect the electrical resistivity. The compositions with the lower Si content of y = 0.1 have not been included to the graph, to improve readability. The measured differences are within the standard deviation. The large increase of electrical resistivity in Zr-rich alloys reflects the lattice distortion from the above-mentioned XRD analyses.

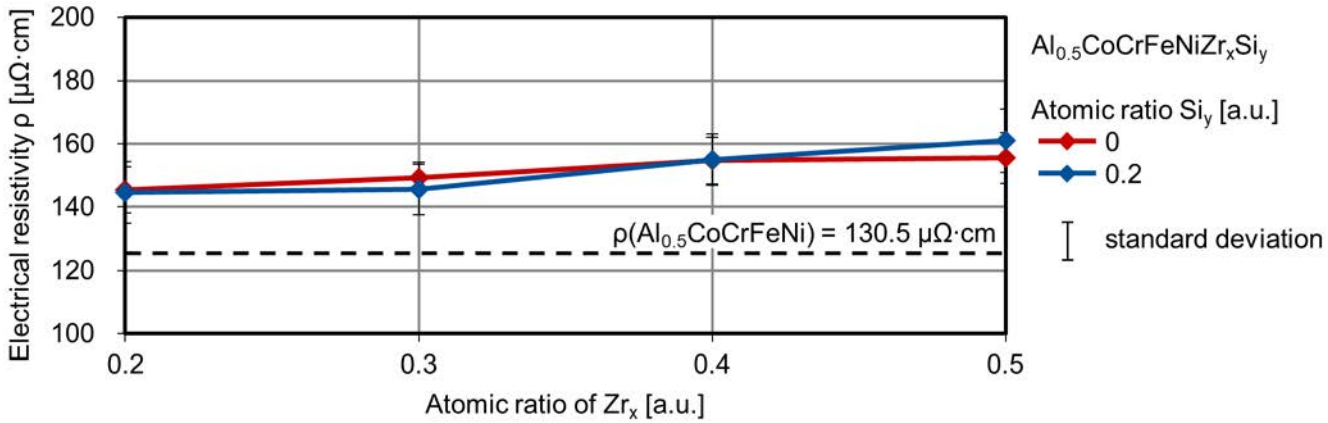

Figure 2. Measured electrical resistivity of $Al_{0.5}CoCrFeNiZr_xSi_y$ alloys in comparison to $Al_{0.5}CoCrFeNi$.

To predict the lifetime of the HEA in application as heating coatings, thermal aging in air for cumulative 324 h at 600 °C was conducted. From the thermal aging, a general trend was observed that the higher the Zr content of the alloys the more oxidized the surfaces were. Additionally, the phase composition in most alloys has changed as well. As an example, the XRD pattern of $Al_{0.5}CoCrFeNiZr_{0.5}$ with the highest Zr content is given on the left side of Figure 3. First changes of the phase composition have been detected as early as after the first aging period of

24 h. After the cumulative 324 h of aging, one significant difference is the change from mainly bcc to mainly fcc phase over time. Many phases of minor quantities were formed, of which the oxide Fe_3O_4 with the JCPDS card 01-072-6170 is the most dominant one. This severe change in phase composition and level of oxidation at elevated temperatures reduces the alloy's prospects in the application as heating element. A promising result, though, was detected with the composition $Al_{0.5}CoCrFeNiZr_{0.2}Si_{0.2}$, which is demonstrated on the right side. The phase composition shows only a slightly more pronounced fcc phase, but no major change after a cumulative aging time of 324 h at 600 °C can be detected. Therefore, leading to the assumption that Si stabilizes the phase composition even at elevated temperatures. This is supported by the strongly exothermic mixing of Si with the other components within the alloy according to the mixing enthalpies calculated by Takeuchi and Inoue [17]. Additionally, the cumulated mass proportion of Al, Cr and Si is the highest in $Al_{0.5}CoCrFeNiZr_{0.2}Si_{0.2}$ with 27.2 wt.-%, if compared to the other investigated compositions. As these elements are commonly known to form stable oxide layers, it is assumed that this is another factor towards the observed results. Even though $Al_{0.5}CoCrFeNiZr_{0.2}Si_{0.2}$ exhibits only a 10 % increase of the electrical resistivity compared to $Al_{0.5}CoCrFeNi$, the phase stability is of particular importance to the application as heating coating. With this auspicious phase stability the long term application as a heating element without failure seems feasible.

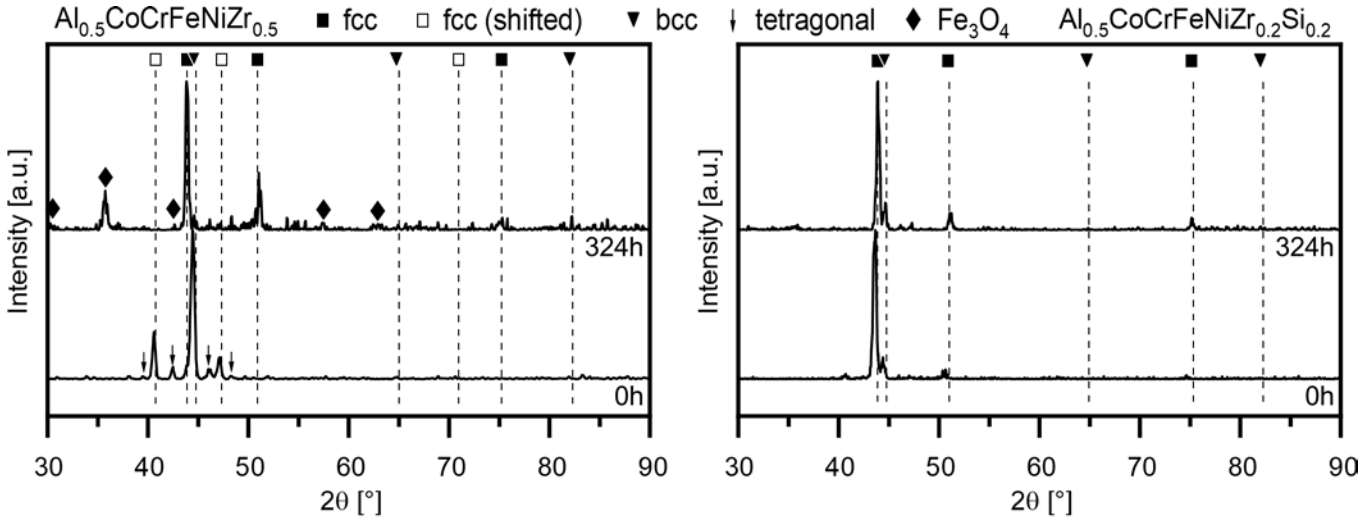

Figure 3. XRD analyses of $Al_{0.5}CoCrFeNiZr_{0.5}$ (left) and $Al_{0.5}CoCrFeNiZr_{0.2}Si_{0.2}$ (right) before and after ageing for 324 h at 600 °C.

Thermally sprayed coatings, however, exhibit a differing microstructure, when compared to ingots of the same composition. Therefore, the anisotropic microstructure of thermally sprayed coatings and extremely high cooling rates of the splats during thermal spraying are approximated by producing tapes by means of melt spinning. Unfortunately, melt spinning of the different HEA compositions turned out to be an outstanding challenge. While the composition $Al_{0.5}CoCrFeNi$ without Zr and Si resulted in perfectly shaped tapes, the quality of the tapes was scattered in a wide range as seen in Figure 4. As Zr is an element, which is commonly used in active brazing to join ceramics, the Zr-rich alloys were expected to be difficult to process. However, even a tape was produced successfully from the highest Zr-content alloy $Al_{0.5}CoCrFeNiZr_{0.5}$. While the tape with the lowest combined content of Zr and Si, $Al_{0.5}CoCrFeNiZr_{0.2}Si_{0.1}$, formed a usable tape, all other combination of Zr and Si addition have failed so far. This leads to the assumption that some interactions between Zr and Si increases the chemical reactivity of the alloys, and is followed by a reaction with the crucible made from BN. For the focus in this work, the successfully produced tapes were analyzed further, while the investigation regarding the melt spinning of the other alloys is ongoing. At this point, it has to be pointed out that the promising alloy $Al_{0.5}CoCrFeNiZr_{0.2}Si_{0.2}$ could not be produced as tape as seen in the bottom right corner of Figure 4. Instead, $Al_{0.5}CoCrFeNiZr_{0.2}Si_{0.1}$ was included in the following comparison of electrical resistivity. It exhibits the most similar chemical composition, although its phase composition after thermal aging experienced a significant change.

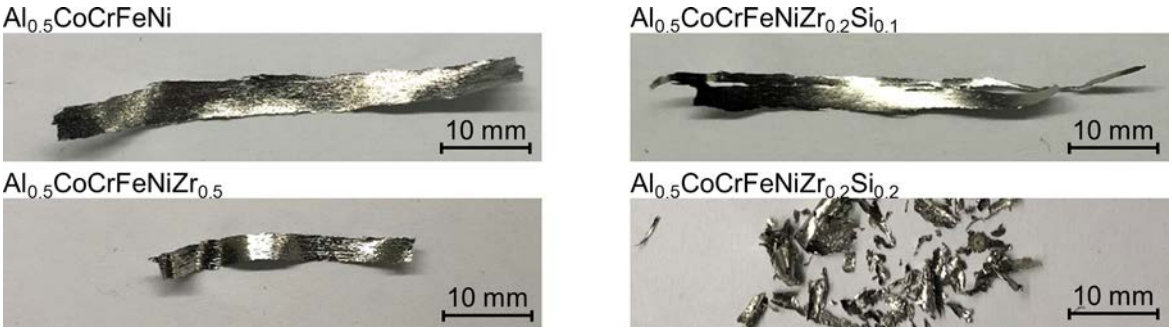

Figure 4. Melt-spun tapes of selected $Al_{0.5}CoCrFeNiZr_xSi_y$ alloys.

The achieved results of the electrical resistivity of melt-spun tapes, however, gives a highly promising outlook as illustrated in Figure 5. The electrical resistivity of melt-spun tapes is significantly higher than the one of their corresponding ingots. This is attributed to the rapid solidification in the melt spinning process, which leads to much smaller grain sizes, and therefore increases the amount of grain boundaries. These boundaries act as additional resistance for electron movement, if compared to a single crystal. Paired with the existence of up to seven elements, the rapid solidification may lead to an amorphous phase, which due to its high level of disorder may affect the electrical resistivity as well. A similar trend is expected to be observed for thermally sprayed coating from these HEA.

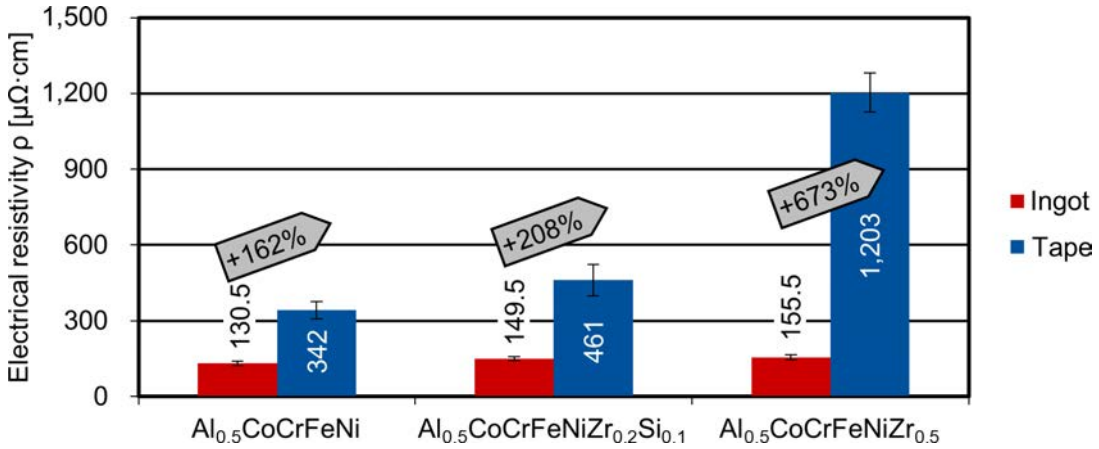

Figure 5. Electrical resistivity of melt-spun tapes in comparison to their corresponding ingot.

4 Conclusion

HEA with 13 differing compositions in the system $Al_{0.5}CoCrFeNiZr_xSi_y$ were produced from powder mixtures by means of remelting in a vacuum furnace. The addition of Zr significantly increases the electrical resistivity of the alloys, while the addition of Si has no considerable effect on the electrical resistivity. Therefore, the intended distortion of the lattice of the reference alloy $Al_{0.5}CoCrFeNi$ was achieved by addition of Zr. However, in future application of these HEA as heating elements, not only a high electrical resistivity of the alloy but also phase stability at elevated temperatures is essential. With $Al_{0.5}CoCrFeNiZr_{0.2}Si_{0.2}$, a HEA was developed, which shows promising phase stability up to 600 °C, while providing an electrical resistivity of 144.5 μΩ·cm, which is an improvement of more than 10 % compared to $Al_{0.5}CoCrFeNi$ and even more than 30 % compared to the state-of-the-art heating element alloy NiCr20. First investigations of melt spun tapes show highly promising electrical resistivity, which are more than double the value of the corresponding ingots' electrical resistivity. Due to the rapid solidification during the melt spinning process, these tapes approximate the structure of a thermally sprayed coating more precisely. Therefore, a stronger focus should be set on their investigation in the future.

In summary, with its high electrical resistivity and promising phase stability up to 600 °C, $Al_{0.5}CoCrFeNiZr_{0.2}Si_{0.2}$ presents itself as an auspicious alternative to current heating element alloys. The current research shows no thermal limitation for HEA in the application of injection moulding of plastics, where typically temperatures of up to 300 °C occur.

Acknowledgements

The presented investigations were carried out at RWTH Aachen University within the framework of the project Entwicklung neuartiger metallischer Zusatzwerkstoffe für Heizelemente mittels Thermischen Spritzens

(BO 1979/76-1, 437095503) and funded by the Deutsche Forschungsgemeinschaft e.V. (DFG, German Research Foundation). The sponsorship and support are gratefully acknowledged.

Literature

[1] J. Giessauf, G. Pillwein, G. Steinbichler, Werkzeugtemperierung: Die variotherme Temperierung wird produktionstauglich (Mold Temperature Control: Variotherm Temperature Control Is Fit for Production), Kunststoffe 98 (2008) 87–92.
[2] M. Fasching, F.B. Prinz, L.E. Weiss, “Smart” Coatings: A Technical Note, Journal of Thermal Spray Technology 4 (1995) 133–136.
[3] M. Prudenziati, Development and the Implementation of High-Temperature Reliable Heaters in Plasma Spray Technology, J Therm Spray Tech 17 (2008) 234–243. https://doi.org/10.1007/s11666-008-9164-6.
[4] M. Prudenziati, M.L. Gualtieri, Electrical Properties of Thermally Sprayed Ni- and Ni20Cr-Based Resistors, J Therm Spray Tech 17 (2008) 385–394. https://doi.org/10.1007/s11666-008-9187-z.
[5] M. Floristán, R. Fontarnau, A. Killinger, R. Gadow, Development of electrically conductive plasma sprayed coatings on glass ceramic substrates, Surface and Coatings Technology 205 (2010) 1021–1028. https://doi.org/10.1016/j.surfcoat.2010.05.033.
[6] S. Scheitz, F.-L. Toma, L.-M. Berger, R. Puschmann, V. Sauchuck, M. Kusnezoff, Thermally sprayed multilayer ceramic heating elements, Thermal Spray Bulletin 11 (2011) 88–92.
[7] K. Bobzin, W. Wietheger, M.A. Knoch, A. Schacht, Heating behaviour of plasma sprayed TiOx/Cr2O3 coatings for injection moulding, Surface and Coatings Technology 399 (2020) 126199. https://doi.org/10.1016/j.surfcoat.2020.126199.
[8] D. Fritsche, C. Hopmann, C.E. Kahve, T. Hohlweck, K. Bobzin, H. Heinemann, A. Schacht, Einsatz und Einflussnahme von thermisch gespritzten Heizschichten im variothermen Spritzgießprozess, In Proceedings: Technomer 2021 - 27. Fachtagung über Verarbeitung und Anwendung von Polymeren, 04.-05.11.2021, Chemnitz (2021).
[9] J.-W. Yeh, S.-K. Chen, S.-J. Lin, J.-Y. Gan, T.-S. Chin, T.-T. Shun, C.-H. Tsau, S.-Y. Chang, Nanostructured High-Entropy Alloys with Multiple Principal Elements: Novel Alloy Design Concepts and Outcomes, Adv. Eng. Mater. 6 (2004) 299–303. https://doi.org/10.1002/adem.200300578.
[10] M.C. Gao, J.-W. Yeh, P.K. Liaw, Y. Zhang, High-Entropy Alloys, Springer International Publishing, Cham, 2016.
[11] H.-P. Chou, Y.-S. Chang, S.-K. Chen, J.-W. Yeh, Microstructure, thermophysical and electrical properties in AlxCoCrFeNi (0≤x≤2) high-entropy alloys, Materials Science and Engineering: B 163 (2009) 184–189. https://doi.org/10.1016/j.mseb.2009.05.024.
[12] Y.-F. Kao, S.-K. Chen, T.-J. Chen, P.-C. Chu, J.-W. Yeh, S.-J. Lin, Electrical, magnetic, and Hall properties of AlxCoCrFeNi high-entropy alloys, Journal of Alloys and Compounds 509 (2011) 1607–1614. https://doi.org/10.1016/j.jallcom.2010.10.210.
[13] R.A. Serway, J.W. Jewett, Principles of Physics, Saunders College Pub., Forth Worth, Texas, 1998.
[14] L. Chen, Z. Zhou, Z. Tan, D. He, K. Bobzin, L. Zhao, M. Öte, T. Königstein, High temperature oxidation behavior of Al0.6CrFeCoNi and Al0.6CrFeCoNiSi0.3 high entropy alloys, Journal of Alloys and Compounds 764 (2018) 845–852. https://doi.org/10.1016/j.jallcom.2018.06.036.
[15] L. Chen, K. Bobzin, Z. Zhou, L. Zhao, M. Öte, T. Königstein, Z. Tan, D. He, Effect of Heat Treatment on the Phase Composition, Microstructure and Mechanical Properties of Al0.6CrFeCoNi and Al0.6CrFeCoNiSi0.3 High-Entropy Alloys, Metals 8 (2018) 974. https://doi.org/10.3390/met8110974.
[16] W.-R. Wang, W.-L. Wang, S.-C. Wang, Y.-C. Tsai, C.-H. Lai, J.-W. Yeh, Effects of Al addition on the microstructure and mechanical property of AlxCoCrFeNi high-entropy alloys, Intermetallics 26 (2012) 44–51. https://doi.org/10.1016/j.intermet.2012.03.005.
[17] A. Takeuchi, A. Inoue, Calculations of Mixing Enthalpy and Mismatch Entropy for Ternary Amorphous Alloys, Materials Transactions 41 (2000) 1372–1378. https://doi.org/10.2320/matertrans1989.41.1372.